X-Ray Spectroscopic Measurements of High Densities and Temperatures from Indirectly Driven Inertial Confinement Fusion Capsules

B. A. Hammel, C. J. Keane, M. D. Cable, D. R. Kania, J. D. Kilkenny, R. W. Lee, and R. Pasha
Lawrence Livermore National Laboratory, Livermore, California 94550
(Received 21 August 1992)

Time-resolved x-ray spectroscopy is used to study the implosion of indirectly driven inertial confinement fusion capsules on the Nova laser. Through the use of Ar dopant in the fuel, measurements of the peak temperature, from emission line ratios, and density, from line broadening, are obtained. These measurements indicate peak electron temperatures of ~ 1–1.6 keV and electron and deuteron densities in the range of $(1.0$–$2.0)\times 10^{24}$ cm^{-3}, depending on the type of laser drive used. These ion densities, which approach those of stellar interiors, are the highest inferred by direct analysis of Stark-broadened line profiles.

PACS numbers: 52.25.Nr, 32.70.−n, 52.50.Jm, 52.70.La

Direct observations of ultrahigh densities are limited to a small class of physical phenomena. For example, although high densities occur in stellar interiors ($n_i \sim 10^{24}$–10^{26} cm^{-3}), direct observation of these conditions requires the detection of neutrinos which can escape the core of the star [1]. Conditions in laser-driven inertial confinement fusion capsules approach those of stellar interiors, and provide a unique opportunity to directly observe matter at ultrahigh densities and high temperatures. X-ray spectroscopic measurements of the compressed core conditions of directly driven inertial confinement fusion (ICF) capsules, which are filled or doped with high-Z gas, have been performed by a number of researchers [2–7]. In the work presented here, time-resolved x-ray spectroscopic measurements of the compressed core of indirectly driven ICF capsules are used to infer conditions in the deuterium fuel [8]. By seeding the fuel with Ar, we infer the fuel density from measurements of the Stark-broadened He-$\beta(n=3\text{-}1)$ line profiles, and the electron temperature from the ratio of Ly-β to He-β. These measurements indicate peak core electron temperatures of ~ 1–1.6 keV and electron and deuteron densities in the range of $(1.0$–$2.0)\times 10^{24}$ cm^{-3}, depending on the type of laser drive used. These ion densities, which approach those of stellar interiors, are the highest ascertained by direct analysis of Stark-broadened line profiles. Since at these high densities $T_e \sim T_i$, the measured ion energy density $n_i T_i$, which is relevant for achieving high fusion rates, is $\sim (1$–$2)\times 10^{27}$ eV/cm^3.

These ICF capsules are indirectly driven using the Nova laser [9]. The capsules are made of plastic and are contained within a cylindrical gold hohlraum of millimeter scale (Fig. 1). The ten beams of the Nova laser are directed into the hohlraum, producing a uniform x-ray flux which ablatively drives the capsule. Both the shape and total energy of the laser pulse can be varied, allowing the drive to be optimized to the particular capsule. The pulse shape used in these experiments was either a flat-topped laser pulse with a 1-ns duration or a shaped pulse, consisting of a low-power "foot" followed by a peak at 3 times the power, and an overall duration of 2.2 ns. For the 1-ns experiments, the total energy in the pulse was either 12 kJ (low drive), 19 kJ (medium drive), or 25 kJ (high drive) of 353-nm light. The shaped pulse had a total energy of 27 kJ and a peak power of 20 TW. The capsules are filled with deuterium and doped with Ar (0.1 at.%). The low concentration of Ar implies that the electron and ion densities in the fuel are essentially equal ($n_e \simeq n_i \equiv n_{e,i}$).

In our experiments we have minimized the amount of Ar, to insure that it is nonintrusive and that the diagnostic lines are optical thin. The optical depth of a line can be written as $(F_{\mathrm{He}} b/M_{\mathrm{D}})[(\pi e^2/mc) f\phi(E)]\rho R_D$, where b is the Ar fraction by number (10^{-3}), F_{He} is the fraction of Ar ions that are in a particular ion state ($\sim 50\%$ He-like, 50% H-like), M_{D} is the mass of a deuterium atom, and ρR_D refers to the peak fuel areal mass density. The term in square brackets is the absorption cross section which, for our conditions, has a calculated maximum value of 2.3×10^{-19} cm^2 for Ar He-β. The peak fuel areal density for these implosions, from secondary neutron measurements [10], is ~ 5–10 mg/cm^2, resulting in a maximum optical depth of between 0.2 and 0.4 in the Ar He-β line. The absorption cross section for the Ly-β line is 2.9×10^{-19} cm^2; hence its optical depth is also 0.2–0.4.

Measurements of the x-ray emission from the Ar dopant are made with two streaked x-ray crystal spectrometers [8]. One crystal spectrometer provides survey

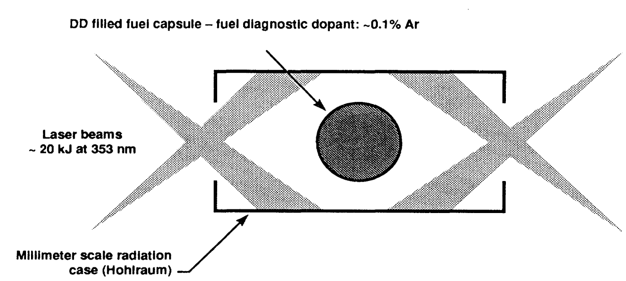

FIG. 1. Schematic diagram of indirectly driven capsule in a hohlraum.

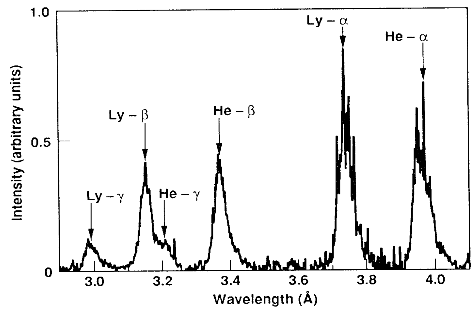

FIG. 2. Measured Ar spectra from an indirectly driven capsule, obtained using the survey spectrometer. Continuum is subtracted and lines are fitted to determine linewidths and intensity ratios.

spectra, with a spectral resolving power $\lambda/\Delta\lambda$ of 500–1000 depending on the spectral region under study. The second instrument provides higher-resolution spectra ($\lambda/\Delta\lambda$ of 1500–3000) for detailed studies of line shapes. The survey spectrometer uses a flat RAP crystal and has a dispersion on film of $\sim$0.44 Å/cm, and a simultaneous spectral coverage of approximately 1.3 Å. The high-resolution spectrometer was operated with a flat PET crystal resulting in a dispersion on film of 0.127 Å/cm, and a simultaneous coverage of $\sim$0.4 Å. The spectrometers are coupled to x-ray streak cameras. The cameras use either CsI or Au photocathodes, depending on the sensitivity requirements. An ITT image intensifier (F4113), coupled to the streak camera, is used to increase the sensitivity of the system. Data are recorded on 35-mm film. This instrument provided $\sim$35-ps temporal resolution for these measurements. Observed spectra are corrected for the film, filters, and photocathode response. Only conditions corresponding to peak compression are reported here.

A typical spectrum at peak compression, taken with the survey spectrometer, from an Ar-doped capsule includes transitions from He- and H-like ion stages, as shown in Fig. 2. The $n=2$-1 transitions (He-α and Ly-α) are optically thick ($\tau \sim 10$), and therefore of limited use. The $n=3$-1 transitions (He-β and Ly-β) are optically thin, and provide a means of determining both the density and electron temperature of the compressed fuel. Using measurements of the Stark-broadened He-β line profile, we infer the fuel density by using standard line-broadening theory, in which the ions and electrons are treated in the quasistatic and impact approximation, respectively [11, 12]. Doppler broadening is also included. He-β is preferred for the measurement of density due to the blending of Ly-β and He-γ ($n=4$-1).

Typical spectral line shapes of the He-β line are shown in Fig. 3. For implosions with a 1-ns medium drive laser pulse, the He-β line typically reaches a width of 30 ± 5 mÅ (33 eV). Implosions using the shaped laser pulse result in greater observed broadening of the He-β line, 50 ± 8 mÅ (55 eV). The inferred field density for these two drive conditions, based on published calculations of the width of the He-β line as a function of density [12], are $n_{e,i}=(1.2\pm0.3)\times10^{24}$ cm^{-3} and $n_{e,i}=(2.3\pm0.5)\times10^{24}$ cm^{-3}. Higher peak densities are expected on implosions driven by shaped laser drive, due to the more isentropic compression of the fuel. The errors in the inferred densities are due to noise in the time-resolved measurements. This noise is statistical in nature, due to the low signal levels, and typically results in 10%–20% errors in the width of a line.

The line profiles shown in Fig. 3 appear somewhat asymmetric, with an enhancement in the intensity on the long-wavelength side of the line, typical of a line with satellites arising from doubly excited states. Calculations of the He-β line profile, including the effects of the Stark-broadened Li-like satellites of the type $1s2l3l'$-$1s^22l$ and $1s3l3l'$-$1s^23l$, have been performed, and show

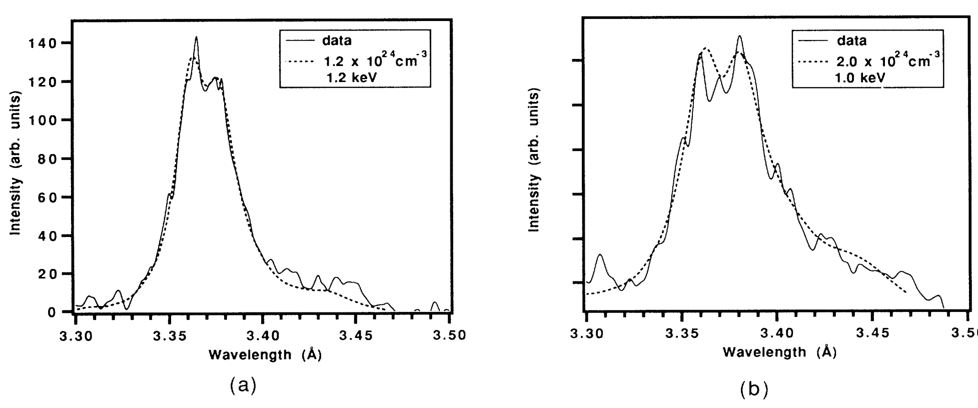

FIG. 3. (a) He-β line profile for a 1-ns flat-top and (b) 2.2 ns, 3:1 contrast pulse-shaped drive showing increased broadening due to higher peak fuel densities. Measured line profiles are shown as solid lines while calculated line profiles are dashed lines. Calculations assume $n_{e,i}=1.2\times10^{24}$ cm^{-3}, $T_e=1.2$ keV for the 1-ns drive and $n_{e,i}=2.0\times10^{24}$ cm^{-3}, $T_e=1.0$ keV for the shaped drive, and include the effect of satellites of the type $1s2l3l'$-$1s^22l$ and $1s3l3l'$-$1s^23l$. These data were obtained using the survey spectrometer.

a dramatic effect on the width of the He-β line at low temperatures [13–15]. To avoid an overestimate of the density, we must account for the effect of satellites in our observations. In Fig. 3, we show fits of calculated profiles [using non-LTE (local thermodynamic equilibrium) populations] from the TOTAL code [16], to the data. The electron temperature is consistent with the temperature inferred from the ratio of Ly-β to He-β, described below (1.2 keV for the 1-ns drive and 1.0 keV for the shaped drive). The inferred density for the 1-ns flat-top drive case is $n_{e,i}=(1.2\pm0.3)\times10^{24}$ cm^{-3}, unchanged from the above value based solely on the width. The inferred density for the shaped drive pulse is $n_{e,i}=(2.0\pm0.5)\times10^{24}$ cm^{-3}, somewhat lower than the above value. This is reasonable due to the larger satellite contribution at lower fuel temperatures. The calculated profiles shown in Fig. 3 include a 5 mÅ instrumental width.

The measurements and calculations in Fig. 3 agree quite well. No evidence of a dip at line center is observed, in agreement with the calculated line profile which includes the effect of the instrumental resolution. To reduce the role of the instrumental width, we measured this line shape with the high-resolution spectrometer. A spectrum at peak compression, from a 1-ns high drive capsule, is shown in Fig. 4. No evidence of a central dip is observed in this data either, even though the resolution is ~1.5 mÅ. This is in contrast to the calculated line shape, also shown in the figure, with $n_{e,i}=1.2\times10^{24}$ cm^{-3}, $T_e=1.55$ keV, and a 1.5 mÅ instrumental width, where the improved instrumental resolution results in an obvious dip. Calculations which include ion dynamics predict a reduction of the central dip [17,18]. However, gradients in the density may also contribute to the filling in of the central dip. Since, in our experiments, the perturbing fields are due to deuterons, the effects of ion motion are greater than in previous work with pure Ar fills, where a dip has been observed [2]. Indeed, recent calculations for conditions similar to ours show substantial filling in of the dip [19]. Despite this qualitative agreement, an unambiguous measurement of the effects of ion motion on the line profile will require further experiments. In addition, it is interesting to note that there is an apparent shift of the central wavelength of this line, from its initial position (3.365 Å) toward longer wavelength by ~10 mÅ. Shifts in line position due to perturbing ions and electrons are predicted by calculation [18], although other effects could lead to our result (including instrumental effects). This shift will be addressed in greater detail in future experiments.

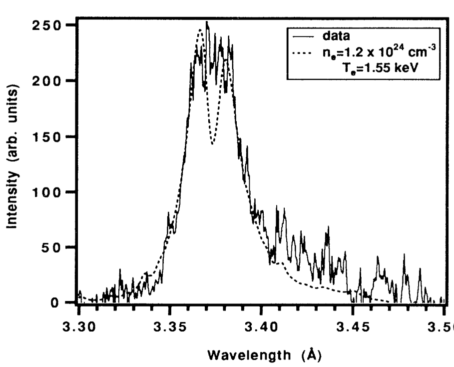

FIG. 4. Measured high-resolution He-β line profile for 1-ns "high drive" implosion compared to the calculated line profile at $n_{e,i}=1.55\times10^{24}$ cm^{-3}, $T_e=1.55$ keV. The resolution is 1.5 mÅ.

We used the Ar Ly-β/He-β ratio to infer the fuel electron temperature for implosions driven by the laser pulse shapes described above. For the three 1-ns flat-top drive conditions we measured the resulting change in this line ratio, as shown in Fig. 5. The temperatures were obtained from calculations using a collisional radiative equilibrium code [20], and are shown next to the data. Since this ratio is also weakly dependent on density, we deduced these temperatures by calculating the ratio using the densities from the Stark-broadening measurements. The assumption of steady-state ionization is justified because of the high electron densities present. As can be seen from Fig. 5, the temperature inferred from the ratio of the Ly-β and He-β lines increases as the drive energy increases. This is in qualitative agreement with expectations and modeling [15]: Increased capsule drive should result in higher implosion velocities and, hence, higher fuel temperatures. This ratio was also measured on capsules driven with the 3:1 contrast laser pulse. We observed Ly-β/He-β=0.4, corresponding to $T_e=1.00$ keV. In these measurements, errors of $\pm20\%$ in this ratio, due to noise in the data, lead to an uncertainty in the inferred electron temperature of $\sim\pm50$ eV. This measurement represents an "average" temperature of the core over the emitting volume, weighted by emissivity. Ion temperature measurements, from neutron time-of-flight analysis, are consistently higher than the measured electron temperature by 30%–40% [21].

Spectroscopic observations of high electron densities in laser compressed capsules have been reported in previous publications [2–7]. In the most recent of these works, Hooper *et al.* [7], time-resolved spectra from directly driven capsules filled with pure Ar are fitted with calcu-

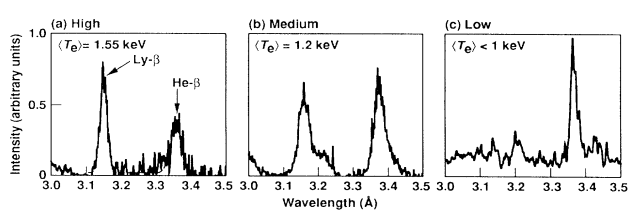

FIG. 5. Measured Ar Ly-β and He-β lines for (a) "high-" (b) "medium-," and (c) "low-power" 1-ns drives. Inferred average fuel electron temperatures $\langle T_e\rangle$ from the RATION code are shown next to the data.

lated line shapes. Our results differ from those of Hooper *et al.* in several important respects. First, since their capsules contained only Ar, their highest estimates of the electron density correspond to ion densities of $\sim 4\times 10^{23}$ cm^{-3}. Second, since the electron temperature achieved in their implosions, at these densities, is $\sim$650 eV, the energy density of the ions $(n_i T_i)$ is $\sim 2.6\times 10^{26}$ eV/cm^3. Finally, it is important to note that the results presented here offer significant improvements in the accuracy of the measurements of density and temperature over those of Hooper *et al.* The results in Ref. [7] use detailed modeling including kinetics, line shape, and radiative transfer effects to produce fits to the observed He-α and Ly-α line profiles and associated satellites and infer electron density and temperature. The technique of Hooper *et al.* is much less sensitive to electron density than that described in the present work. This can be clearly seen in Fig. 4 of Ref. [7], where variations of up to a factor of 8 in electron density result in calculated profile differences not substantially larger than typical errors (10%–20%) in streak camera measured line profiles. This presumably arises due to the strong opacity broadening ($\sim$16 optical depths on Ly-α and $\sim$33 depths on He-α) present in the data of Ref. [7]. In marked contrast, the present analysis relies on the width of the optically thin He-β line, which scales roughly as $n_e^{2/3}$. Hence, a factor of 8 in density results in a factor of 4 in the width of the line.

It is a pleasure to acknowledge the contributions of R. J. Wallace to this work. We gratefully acknowledge the work of N. D. Delamater and discussions with R. Mancini and C. Hooper on the inclusion of Li-like satellites to the He-β line shape, and the contributions of J. Nash to the calculations of the non-LTE populations. We thank H. Griem and C. Hooper for many stimulating discussions and for reviewing an early draft of the manuscript.

[1] D. Dearborn, G. Marx, and I. Ruff, Prog. Theor. Phys. **77**, 12 (1987); C. Iglesias and F. Rogers, Astrophys. J. **371**, 908 (1991).
[2] B. Yaakobi, S. Skupsky, R. L. McCrory, C. F. Hooper, H. Deckman, P. Bourke, and J. M. Soures, Phys. Rev. Lett. **44**, 1072 (1980).
[3] A. Hauer, K. B. Mitchell, D. B. van-Hulstyen, T. H. Tan, E. J. Linnebur, M. M. Mueller, P. C. Kepple, and H. R. Griem, Phys. Rev. Lett. **45**, 1495 (1980).
[4] J. D. Kilkenny, R. W. Lee, M. H. Key, and J. G. Lunney, Phys. Rev. A **22**, 2746 (1980).
[5] C. F. Hooper, Jr., R. C. Mancini, D. P. Kilcrease, L. A. Woltz, M. C. Richardson, D. K. Bradley, and P. A. Jaanimagi, Proc. SPIE Int. Soc. Opt. Eng. **913**, 129 (1988).
[6] B. Yaakobi, D. M. Villeneuve, M. C. Richardson, J. M. Soures, R. Hutchison, and S. Letzring, Opt. Commun. **43**, 343 (1982).
[7] C. F. Hooper, D. P. Kilcrease, R. C. Mancini, L. A. Woltz, D. K. Bradley, P. A. Jaanimagi, and M. C. Richardson, Phys. Rev. Lett. **63**, 267 (1989).
[8] B. A. Hammel, C. J. Keane, D. R. Kania, J. D. Kilkenny, R. W. Lee, R. Pasha, and R. E. Turner, Rev. Sci. Instrum. **63**, 5017 (1992).
[9] E. M. Campbell, Laser Part. Beams **9**, 209 (1991). See also John D. Lindl, Robert L. McCrory, and E. Michael Campbell, Phys. Today **45**, No. 9, 32 (1992).
[10] M. D. Cable and S. P. Hatchett, J. Appl. Phys. **62**, 2233 (1987).
[11] R. W. Lee, J. Quant. Spectrosc. Radiat. Transfer. **40**, 560 (1988).
[12] C. J. Keane, R. W. Lee, B. A. Hammel, A. L. Osterheld, L. J. Suter, A. Calisti, F. Khelfaoui, R. Stamm, and B. Talin, Rev. Sci. Instrum. **61**, 2780 (1990).
[13] N. D. Delamater, G. Charatis, C. J. Keane, and B. A. Hammel, "Influence of $1s2l3l'$-$1s^22l$ Satellite Lines on Density Determinations from Stark Broadening Analysis," in Proceedings of the Twentieth Anomalous Absorption Conference, Michigan, 1991 (unpublished).
[14] R. C. Mancini, C. F. Hooper, Jr., N. D. Delamater, A. Hauer, C. J. Keane, B. A. Hammel, and J. K. Nash, Rev. Sci. Instrum. **63**, 5119 (1992).
[15] C. J. Keane, B. A. Hammel, A. L. Osterheld, R. W. Lee, D. R. Kania, L. J. Suter, R. C. Mancini, C. F. Hooper, Jr., and N. D. Delamater, in Proceedings of the Fifth International Workshop on Radiative Properties of Hot Dense Matter, 2–6 November 1992, Santa Barbara, California (to be published).
[16] A. Calisti, F. Khelfaoui, R. Stamm, B. Talin, and R. W. Lee, Phys. Rev. A **42**, 5433 (1990).
[17] R. Stamm, B. Talin, E. L. Pollock, and C. A. Iglesias, Phys. Rev. A **34**, 4144 (1986).
[18] Hans R. Griem, Milan Blaha, and Paul C. Kepple, Phys. Rev. A **41**, 5600 (1990).
[19] A. Calisti, L. Godbert, R. Stamm, and B. Talin, in Proceedings of the Fifth International Workshop on Radiative Properties of Hot Dense Matter (Ref. [15]).
[20] R. W. Lee, B. L. Whitten, and J. E. Strout III, J. Quant. Spectrosc. Radiat. Transfer. **32**, 91 (1984).
[21] B. A. Remington, R. A. Lerche, and M. D. Cable, Rev. Sci. Instrum. **61**, 3128 (1990).